J. Plasma Physics (2012), vol. 78, part 5, pp. 507–513. © Cambridge University Press 2012
doi:10.1017/S0022377812000190

Experimental evaluation of protons emission from a plasma focus device

M. BHUYAN and S. R. MOHANTY

Centre of Plasma Physics, Institute for Plasma Research, Sonapur, Kamrup 782402, Assam, India
(smrutirm@yahoo.com)

(Received 22 November 2011; revised 18 January 2012; accepted 20 January 2012; first published online 27 February 2012)

Abstract. Solid state nuclear track detectors have been used for measuring axially emitted protons from a 2.2-kJ energy plasma focus device. The flux of the protons emerging out from the pinched plasma column of the plasma focus device has been found to saturate the CR-39 detectors. Aluminum filters have been used to avoid the saturation effect. By varying the aluminum filter thickness as well as the etching time of CR-39 detectors, proton tracks have been analyzed. Proton energy above 200 keV to about 1 MeV has been measured by using different thicknesses of aluminum filters. On increasing the etching hours, the most probable track diameter is found to be shifted from lower to higher values. The track number density decreases on increase of the filter thickness, whereas the track diameters increase linearly with respect to the etching time.

1. Introduction

Solid state nuclear track detectors (SSNTDs) have been used extensively over the last few decades to register various high energy-charged light particles such as protons, deuterons, and alpha particles, as well as heavy ions emitted from accelerators, lasers, and high-temperature plasma (Jager et al. 1985; Sadowski et al. 1994; Clark et al. 2000; Szydlowski et al. 2000, 2004; Mehboob et al. 2006). These are primarily solid materials (polymers, glasses, or crystals) and therefore are quite inexpensive and easy to handle in any environment (Awad et al. 2008). Moreover, the importance of these passive detectors is that these can make a permanent damage or impression of a particle on the material having high homogeneity and isotropy (Sadowski et al. 1994). Nevertheless, their high optical transparency, low susceptibility to electromagnetic radiations, and extreme sensitivity to the charged particles make them quite user-friendly. The main advantage of the usage of these detectors in various fields is due to their high efficiency (∼100%) as well as their longevity in very rugged conditions. Moreover, since these detectors do not need any electronics, these can be used in any high electromagnetic noisy experiments such as high-power pulsed plasma system (Szydlowski 2003). The other benefit of these detectors is that these can safely detect the particles flux of up to 10^9 particles/m^2. Contemporary to other detectors, because of the aforementioned advantages of SSNTD, these have been found to be employed in various fields of nuclear and cosmic ray sciences for discovering new particles and antiparticles, radiation measurements, meteoritic studies, etc. (Szydlowski et al. 2000).

During the past several years, the researchers have employed SSNTD (namely CR-39 and LR-115) to characterize ion emissions from plasma focus (PF) device of various bank energy ranges starting from few joules to megajoules (Szydlowski 2003; Takao et al. 2003; Verma et al. 2008). While investigating ion and neutron emissions from 1-MJ PF device, Szydlowski (2003) observed the fast deuteron fluxes of 10^5 ions/cm^2 emitted downstream along the electrode axis direction and these deuterons had energy of above several dozens of keV. It was, however, observed that the fast deuteron emission was not reproducible from shot to shot and decreased with increase in filling gas pressure. The energy spectra and space-resolved measurements of fusion reaction protons of the D(d,p)T reaction were studied by Jager et al. (1985) in two PF devices (having bank energy of 28 and 280 kJ) by using LR-115A, CR-39, and CR-39/PM-355 covered with Al filters. By putting appropriate Al filters in front of SSNTD detectors, they succeeded to distinguish protons of $E_p \geqslant 2.5$ MeV from deuterons and other fusion products. Moreover, they measured the reaction proton yield of 10^{11} by employing their 2-mm spatial resolution pinhole camera. Szydlowski et al. (2004) discussed in detail the track dimension as a function of ion energy, atomic number, and etching time. The angular and spatial distribution of ions and their mass and energy spectra have been investigated by Sadowski et al. (1999) by employing a host of diagnostics such as SSNTD, ion pinhole camera, and Thomson spectrometer. The ion angular distribution as measured with a set of small SSNTD samples placed upon a semicircular support of 30-cm radius indicated maximum ion flux at an angle of about 20° to z-axis. On the other hand, the ion pinhole camera used by them only registered ion energy above 400 keV because of constraint on the high-pressure zone between the

https://doi.org/10.1017/S0022377812000190 Published online by Cambridge University Press

detector and the pinch column. Further, they noticed the track saturation nearly at the center of the ion picture, and the track density of the order of 10^6 at the periphery. The deuteron spectrum as observed by Thomson spectrometer (Sadowski et al. 1999) is indicative of two components having energy range of 0.3–0.8 MeV (slow one) and above 0.8 MeV (fast one). Szydlowski et al. (2005) reported the measurement of fusion-reaction protons from PF-1000 and TEXTOR tokamak with the help of PM-355 detectors. In order to find out angular distribution and total fusion proton yield from PF-1000, the detectors were mainly placed inside the discharge chamber at the electrode axis, 90° to it. They observed clear differences in the track numbers as well as proton energy in both the directions, which may be due to the moving pinch plasma column.

Most of the earlier works on ion studies from PF device using SSNTD mainly focused on deducing ion energy and flux by overlooking the attenuation of ion during its transportation from the pinch column to detectors. Moreover, a very few earlier works had discussed in detail the saturation effect of SSNTD due to high fluence of ion emission from this device. In the present communication, we have tried our best to address these problems by extracting ions from the very neighborhood of pinch column and by putting ion filters in front of SSNTD to overcome the saturation effect. Basically, we have characterized axially emitted protons by using CR-39 detectors coupled with Al filters. The motivation behind the characterization of proton emission from our PF device is solely the future application of this small proton source for testing materials that are relevant for fusion reactors.

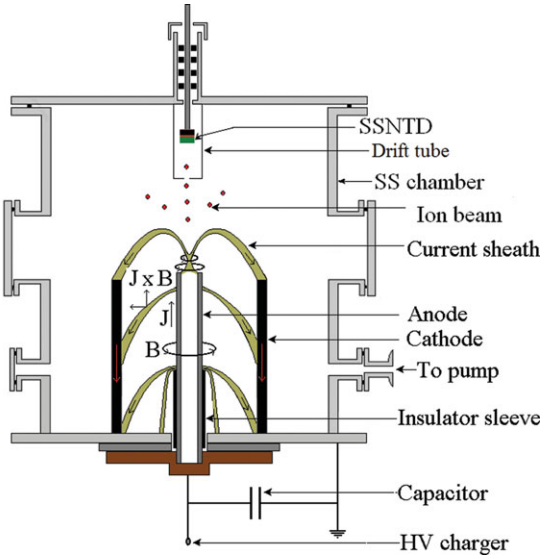


Figure 1. (Colour online) Schematic diagram of the experimental setup.

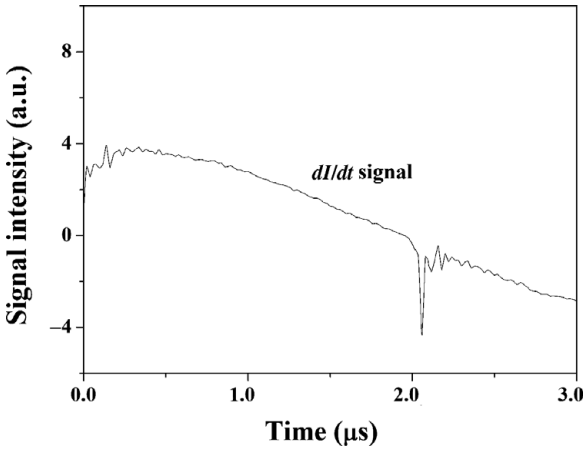


Figure 2. A typical dI/dt signal at optimum pressure.

2. Experimental setup

The proton beam emission was studied from our 2.2-kJ energy PF device (Mohanty et al. 2005) by employing CR-39 detectors. The schematic of experimental setup is shown in Fig. 1 along with the diagnostics. The stainless steel electrode assembly was housed inside a 6-L stainless steel chamber having four viewing ports. The electrodes were separated by a glass insulator sleeve at the bottom. The details of the experimental setup are reported elsewhere (Bhuyan et al. 2004; Mohanty et al. 2005). When the precharged capacitor is discharged across the electrode assembly, the current sheets are developed across the insulator sleeve and these sheaths are axially accelerated down the coaxial electrodes by a self-generated $\mathbf{J} \times \mathbf{B}$ force. At the open end of the electrodes, they undergo radial collapse forming an extremely hot and dense plasma column having a lifetime of 100–200 ns (Mohanty et al. 2005). This plasma column is quite unstable and disrupts due to $m = 0$ instabilities. After disruption of the plasma column, the ions mostly move toward the top of the chamber and electrons go toward the electrode assembly because of the induced electric field together with the self-generated magnetic field.

At 25 kV charging voltage, the capacitor bank delivers a current of 138 kA with a period of 8.4 μs to the load (PF device). The initial inductance up to the initial breakdown path of the insulator is around 250 nH. Usually, the derivative of current (dI/dt) signal is monitored for every PF discharge. A lot of information, such as the focusing quality and gross dynamics of the plasma focus, can be acquired from this signal. A dip in the Rogowski coil signal helps in ascertaining good focusing action in the PF discharge. The working gas pressure at which the maximum dip in the Rogowski coil signal takes place is termed as the optimum pressure for that particular operating gas. The optimum pressure for hydrogen filling gas is 0.3 mm Hg in our case. A typical oscillogram of dI/dt signal recorded at the optimum operating condition is shown in Fig. 2. A sharp singularity in the current derivative indicated the formation of strong plasma focus, which occurs due to

https://doi.org/10.1017/S0022377812000190 Published online by Cambridge University Press

rapid increase of the pinching plasma column inductance at the time of collapsing of the current sheath.

In the present work, the ion emission from hydrogen-filled PF device was carried out by making the space-resolved and time-integrated measurements using CR-39. The CR-39 detector is a colorless rigid plastic with a density of 1.30 g/cm^3. In this work, PM-355 (Pershore Mouldings), a supergrade form of CR-39, was cut into size of 10 × 15 mm^2 and placed inside a drift tube at a height of 7 cm from the top of the anode. The CR-39 detector was placed inside a drift tube at a high vacuum of the order of 7.5 × 10^{-6} mm Hg by making use of a diffusion pump, whereas pressure inside the PF chamber was maintained at 0.3 mm Hg by employing a rotary pump. A 0.5-mm diameter pinhole was used as the entrance of drift tube, which not only collimated the proton beam but also enabled differential vacuum to be maintained between the drift tube and the PF chamber. The entrance pinhole of the drift tube was kept at a height of 3 cm from the top of the anode so that emitted ions of the plasma column suffered minimal attenuation in the background gas medium. After irradiation by the collimated proton beam, the tracks left in the CR-39 material were etched by 6.25 N NaOH solution at 70 ± 2° C for an etching time of 4– 8 h (Tse et al. 2007). The etching solution was mechanically stirred in order to achieve a constant etching condition such as temperature and concentration of the solution. After etching, the detectors were viewed under an Olympus-make optical microscope equipped with a digital scanning fire wire CCD camera. The microscope and CCD camera are interfaced to a computer supporting the Olympus image analysis software. The track images of the detectors were acquired by CCD camera and the images were analyzed using image analysis software. After taking the pictures of the tracks, we randomly selected three different areas (each of 8450.07 μm^2) from that picture. From these three selected areas, the track numbers and diameter were calculated manually and the average value with standard error was estimated. The calculated track numbers per unit area furnish the track number density.

3. Results and discussion

It is well known that when the charged particle strikes the detector medium, it loses energy through the interaction processes like ionization and excitation. The physical quantity that describes the slowing down of charged particles in materials is the stopping power $-dE/dx$, where dE is the energy at distance dx. The energy lost by a particle at distance dx is the energy transferred to the sample (material), so this quantity is called linear energy transfer (LET). The classical expression that describes the specific energy loss is known as the Bethe formula (Knoll 1999) and can be written as follows:

$$-\frac{dE}{dx} = \frac{4\pi e^4 z^2}{m_o v^2} NZ \ln\frac{(2m_o v^2)}{I}.$$

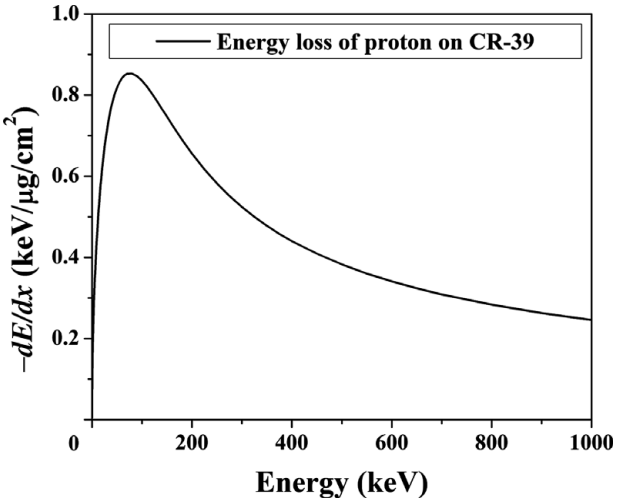


Figure 3. Proton stopping power in the CR-39 detector.

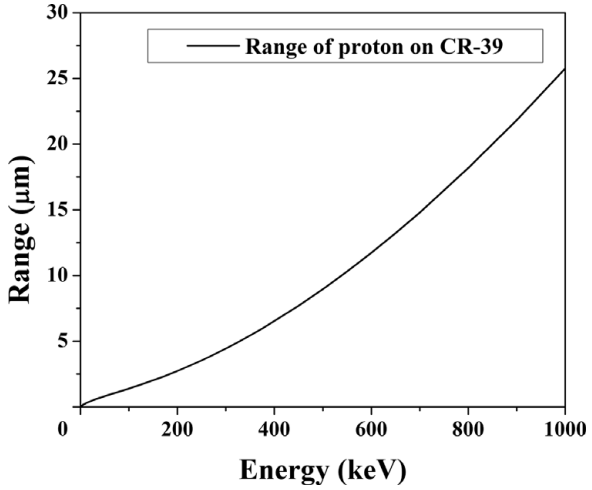


Figure 4. Range–energy relation for proton in the CR-39 detector.

In this expression, v and ze are the velocity and charge of the primary particle, respectively; N and Z are the number density and atomic number, respectively; and m_o is the electron rest mass. Parameter I represents the average ionization and excitation potential of the absorber. The energy loss is inversely proportional to incident particle energy and directly proportional to atomic number. So, energy loss and penetration depth are dependent on particle atomic number and particle energy. Higher atomic number and high-density materials will result in the highest linear stopping power. The stopping power and energy range of the proton can be calculated using the SRIM code (Ziegler et al. 1985). The calculated values of stopping power and energy range are shown in Figs. 3 and 4, respectively.

At first, in order to verify the effect of electromagnetic radiation on track formations in CR-39, we kept the detectors having size of 10 × 15 mm^2 on the top as well as at the side of the chamber, and these detectors were exposed to few PF shots at nonpinching mode of operation, i.e., at higher filling gas pressure. After

https://doi.org/10.1017/S0022377812000190 Published online by Cambridge University Press

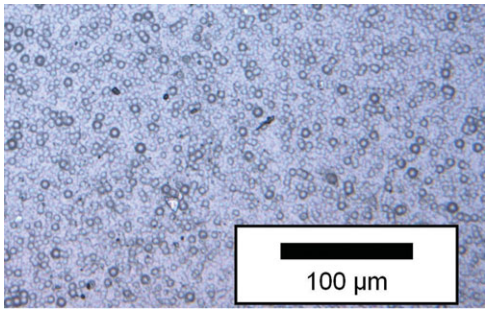


Figure 5. (Colour online) CR-39 exposed to proton in the background.

etching these exposed detectors, we did not find any impression of track on them and thereby confirm that the electromagnetic radiation has no significant effect on CR-39 detectors. Thus, one can safely use such detectors in harsh electromagnetic environments (Sadowski et al. 1999). Next, we have characterized the axially moving proton beam by placing bare CR-39 detectors (without covering the detector by ion filters) at a height of 7 cm from the top of the anode without using the drift tube arrangement. After exposure to PF shots, the etched detectors appear milky white to the naked eye. While viewing under optical microscope, the detector shows the stack of tracks uniformly distributed all around the surface, as shown in Fig. 5. The micrograph indicates that the detectors might have saturated due to high fluence of proton beam (Gaillard et al. 2007). Further, we suspect the role of the scattered proton in the saturation of detectors. Therefore, in order to obstruct the scatter proton from reaching the detectors, we placed the detectors inside the drift tube (as shown in Fig. 1) and thus allowed a well-collimated proton beam to fall on the detector surface. However, after etching, the detectors were still found to be saturated. The systematic study carried out by Gaillard et al. (2007) on saturation of CR-39 detectors reveals that the particle fluences above $\sim 10^8$ particles/cm^2 turn the detector into a saturation regime so that direct track counting is not possible. Thus, as is well known that the particle density of pinch plasma is around 10 orders (Mather et al. 1965) more than that of the saturation limit of CR-39 detector, one can expect the turning of nonopaque detector to milky white due to overexposure, i.e. high fluence of particles. There are quite a few papers on saturation effect in SSNTD due to high fluence of ions. As far as authors' knowledge is concerned, as of now only Castillo et al. (2007) have reported the saturation effect on track detector while detecting the axially moving fusion protons (3.03 MeV). However, they have not reported any way out for overcoming the saturation effect of SSNTD due to high fluence ion emission from the PF device.

We have used a simple technique to overcome the saturation or overlapping effect of CR-39 detectors by covering them with ion filters. Figs. 6(a)–(c) illustrate the typical micrographs of proton tracks of detectors covered with Al filters of 2, 4, and 6 μm. The micrograph

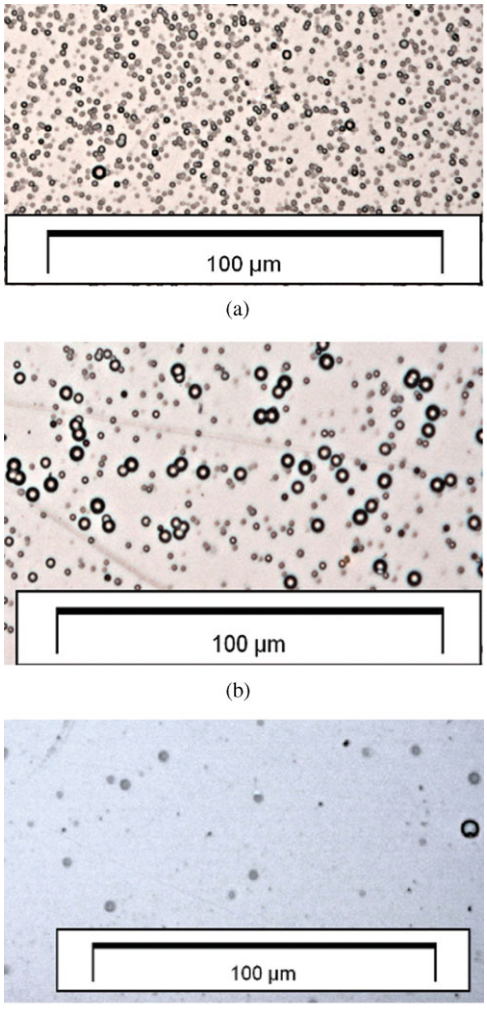


Figure 6. (Colour online) Micrograph of proton track covered with (a) 2 μm, (b) 4 μm, and (c) 6 μm Al filters.

shown in Fig. 6(a) clearly depicts the formation of proton tracks with different diameters, which are uniformly distributed on the surface of the detector. Individual and well-separated tracks are mostly seen in the micrograph along with a few overlapped tracks. Protons of above 220 keV can pass through a 2-μm Al filter (Ziegler et al. 1985) and hence the tracks formed in Fig. 6(a) must be due to the protons of above 220 keV. The dimensions of tracks depend upon the proton energy as well as etching time (Sadowski et al. 1994) and hence different diameters of tracks are suggestive of the emission of polyenergetic protons from the PF device. Nearly circular tracks in the micrographs indicate that the axially emitted protons of PF strike the detector in normal incidence and the tracks induced due to scattered protons might be overruled. The lower limit of proton energy estimation is limited due to the saturation effect of track detector and threshold energy for creation of tracks in CR-39. However, by increasing ion filtration foil thickness, one can easily approximate the upper limit of proton energy estimation. Hence, we have attempted to get a rough estimation of maximum proton energy by putting

https://doi.org/10.1017/S0022377812000190 Published online by Cambridge University Press

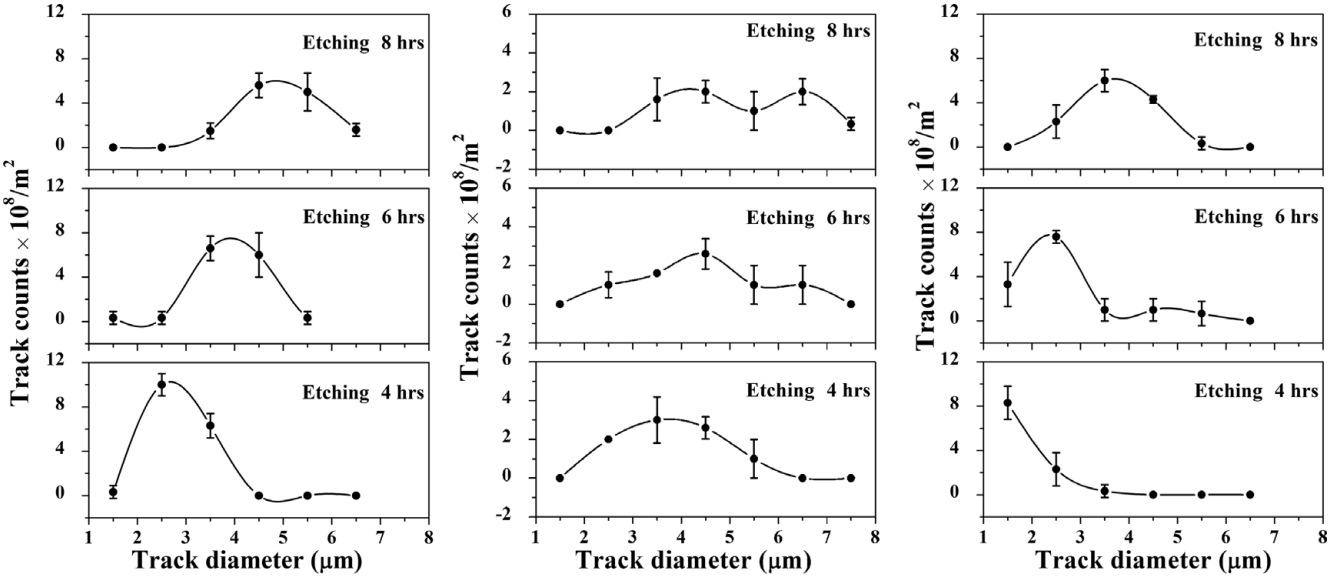


Figure 7. Track density as a function of proton track diameters (a) with 2 μm (b) 4 μm, and (c) 6 μm Al filters.

4–10 μm Al filter in front of the detector. The micrographs of tracks shown in Figs. 6(b) and (c) are still indicative of sufficient number of impressions of proton tracks and the micrograph obtained by covering the detector with 10-μm Al filter (not shown in figure) confirm the emission of proton energy of MeV range. High-energy protons can pass through the material and can make the tracks of small diameter because of small interaction time and small specific energy loss (as $dE/dx \propto 1/E^2$) in terms of energy straggling. On the other hand, low-energy protons follow $dE/dx \propto MZ^2/E$, where E is the incident energy, thus low-energy track sizes were observed (Knoll 1999).

Track density as a function of track diameter at various etching hours has been studied and results are shown in Fig. 7. When we increase etching hours in case of different thicknesses of Al filters, the most probable track diameter has shifted from 2.5 to 4.5 μm, 3.5 to 6.5 μm, and 1.5 to 5 μm in case of 2, 4, and 6 μm Al filters, respectively. This can be explained by the fact that the tracks are etched out to the largest diameter only when the etchant solution enters the end part of the pit without restraint. The etchant has unconstrained access to the end part of the particle trajectory only after removing the external layer of the detector during the etching process. If we increase the etching hours, the etchant material will remove the external layer deeper, resulting in more damaged material area, and as a result the size of the track diameter will be increased. A very interesting feature of all these detection characteristics, i.e., track diameter versus etching time, can be explained by detected particle atomic number and its energy to mass ratios (Szydlowski et al. 2000). After all, this phenomenon is related with the energy loss of the particle on the material or samples and it follows from the fact that dE/dx value of any particle, as well as its

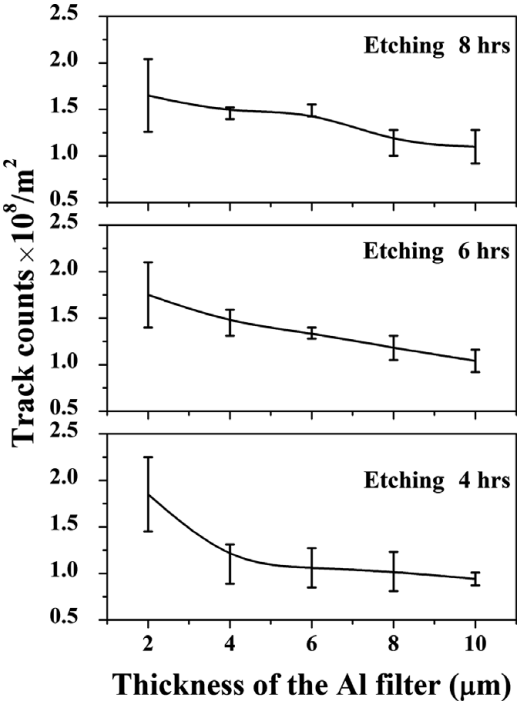


Figure 8. Reduced ion density after passing through various thicknesses of Al filters.

restricted energy loss (REL), is maximum at the end of the range (Szydlowski et al. 2000). Similar results were also observed by Malinowski et al. (2005).

As the proton fluence reduced by using various thicknesses of Al filters, the track number density decreased. This is because, depending on the thickness of the degrader the class of particles exhibiting low energy is not allowed to pass through the medium. On the other hand, the remaining high-energy particles easily pass through the filters and strike the detector. Figure 8 illustrates the track density as a function of thickness

https://doi.org/10.1017/S0022377812000190 Published online by Cambridge University Press

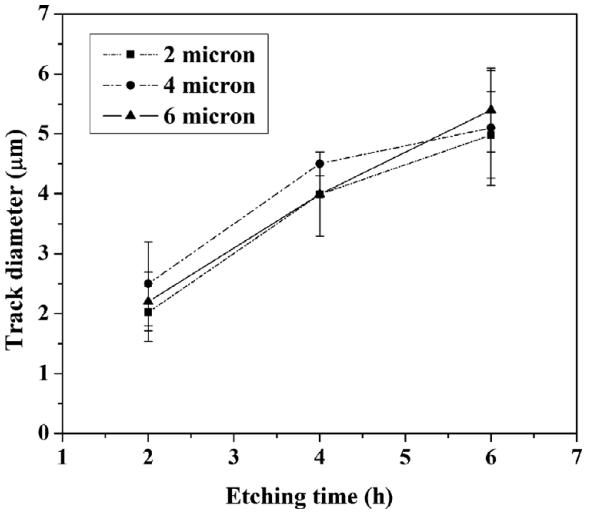


Figure 9. Track diameter as a function of etching hours.

of Al foils (μm) for various etching hours, and it is found to be linearly decreasing in nature. The track diameter evolutions, expressed as a function of etching time, have been presented in Fig. 9. These results are in good agreement with some of the previously reported results (Szydlowski et al. 1999, 2000). These diameters still increase linearly for 4–8 h, although a critical detector layer (equal to the ion range) was removed earlier. Moreover, while carefully analyzing the graph of Fig. 9, one can notice two distinct linear structures, one having between 2 and 4 h and the other being from 4 to 6 h. Higher as well as low-energy protons are contributing to the lower part (from 2 to 4 h) of the graph, whereas only high-energy protons are responsible for the rest part of the graph (above 4 h). A difference in the slope of the two parts can be easily marked from the graph. Our observation of lower slope in case of upper part (above 4 h) is in agreement with the results reported by Szydlowski et al. (2000). They have observed that track diameters rise slower as a function of etching time for high-energy protons.

4. Conclusions

In conclusion, the SSNTDs appear to be very useful for ion diagnostics, typically for PF experiments. The space-resolved and time-integrated characteristics of the proton beam emission from the PF device have been studied by employing CR-39 detectors. The characterization of protons has been done mainly at axial position and have been extracted into the drift tube from the very neighborhood of the pinch column. To remove the saturation effect on the CR-39 detector because of intense proton fluence, the idea of using Al filters in front of the detector has been conceived specifically for our experiment and is well-suited to remove the saturation effect by reducing the fluence of protons. A strong correlation between the dependence of the track density and sizes and the thickness of Al filter and etching hours has been noticed.

Acknowledgments

The authors are grateful to the Director, Institute for Plasma Research, Gandhinagar, India for the financial support to carry out the present work. The technical assistance of M. K. D. Sharma is highly appreciated.

References

Awad, E. M., Soliman, A. A., El-Samman, H. M., Arafa, W. M. and Rammah, Y. S. 2008 Alpha spectroscopy in CR-39 SSNTDs using energy simulation and matrix of energy equations for open field studies. *Phys. Lett.* A **372**, 2959–2966.

Bhuyan, H., Mohanty, S. R., Neog, N. K., Bujarbarua, S. and Rout, R. K. 2004 Comparative study of soft x-ray emission characteristics in a low energy dense plasma focus device. *J. Appl. Phys.* **95**, 2975–2980.

Castillo, F., Herrera, J. J. E., Gamboa, I., Rangel, J., Golzarri, J. I. and Espinosa, G. 2007 Angular distribution of fusion products and x-rays emitted by a small dense plasma focus machine. *J. Appl. Phys.* **101**, 013303.

Clark, E. L., Krushelnick, K., Davies, J. R., Zepf, M., Tatarakis, M., Beg, F. N., Machacek, A., Norreys, P. A., Santala, M. I. K., Watts, I. and Dangore, A. E. 2000 Measurements of energetic proton transport through magnetized plasma from intense laser interactions with solids. *Phys. Rev. Lett.* **84**, 670–673.

Gaillard, S., Fuchs, J., Renard-Le Galloudec, N. and Cowan, T. E. 2007 Study of saturation of CR39 nuclear track detectors at high ion fluence and of associated artifact patterns. *Rev. Sci. Instrum.* **78**, 013304.

Jager, U., Bertalot, L. and Herold, H. 1985 Energy spectra and space-resolved measurements of fusion reaction protons from plasma focus device. *Rev. Sci. Instrum.* **56**, 77–80.

Knoll, G. F. 1999 *Radiation Detection and Measurement*, 3rd edn. New York: John Wiley.

Malinowski, K., Skladnik-Sadowska, E. and Sadowski, M. J. 2005 Comparison of responses of LR-115A, CR-39 and PM-355 track detectors to pulsed low energy proton streams. *Radiat. Meas.* **40**, 371–374.

Mather, J. W. 1965 Formation of a high-density deuterium plasma focus. *Phys. Fluids* **8**, 366–377.

Mehboob, S., Ahmad, S., Waheed, A. and Zakaullah, M. 2006 The nitriding of aluminium by dense plasma focus. *Plasma Sources Sci. Technol.* **15**, 295–301.

Mohanty, S. R., Bhuyan, H., Neog, N. K., Rout, R. K. and Hotta, E. 2005 Development of multi Faraday cup assembly for ion beam measurements from a low energy plasma focus device. *Jpn. J. Appl. Phys.* **44**, 5199–5205.

Sadowski, M., Al-Mashhadani, E. M., Szydlowski, A., Czyzeweski, T., Glowacka, L., Jaskola, M. and Wielunski, M. 1994 Investigation on the response of CR-39 and PM-355 track detectors to protons in the energy range 0.2–4.5 MeV. *Nucl. Instr. Meth. Phys. Res.* B **86**, 311–316.

Sadowski, M., Szydlowski, A., Scholz, M., Kelly, H., Marquez, A. and Lepon, A., 1999 Application of solid state nuclear track detectors for studies of fast ion beams within PF-1000 and other plasma focus facilities. *Radiat. Meas.* **31**, 185–190.

Szydlowski, A. 2003 Application of CR-39 track detectors for corpuscular diagnostics of high-temperature plasma. *Radiat. Meas.* **36**, 35–42.

Szydlowski, A., Banaszak, A., Bienkowska, B., Ivanova-Stanik, I. M., Scholz, M. and Sadowski, M. J. 2004 Measurements

https://doi.org/10.1017/S0022377812000190 Published online by Cambridge University Press

of fast ions and neutrons emitted from PF-1000 plasma focus device. *Vacuum* **76**, 357–360.

Szydlowski, A., Banaszak, A., Sadowski, M. J., Scholz, M. and Wolowski, J. 2005 Advantages of the use of soild-state nuclear track detectors in high-temperature plasma experiments. *Radiat. Meas.* **40**, 479–482.

Szydlowski, A., Sadowski, M., Czyzewski, T., Jaskola, M., Korman, A. and Fijal, I. 2000 Detection characteristics of PM-355 solid-state nuclear track detector for normal incident light ions within MeV energies. *Nucl. Instr. Meth. Phys. Res.* B **171**, 379–386.

Szydlowski, A., Sadowski, M., Czyzewski, T., Jaskola, M. and Korman, A. 1999 Comparison of responses of CR-39, PM-355, and PM-600 track detectors to low energy hydrogen and helium ions. *Nucl. Instr. Meth. Phys. Res.* B **149**, 113–118.

Takao, K., Honda, T., Kitamura, I. and Masugata, K. 2003 Purity of nitrogen ion beams produced in a plasma focus. *Plasma Sources Sci. Technol.* **12**, 407–411.

Tse, K. C. C., Nikezic, D. and Yu, K. N., 2007. Comparative studies of etching mechanisms of CR-39 in $NaOH/H_2O$ and NaOH/ethanol. *Nucl. Instr. Meth. Phys. Res.* B **263**, 300–305.

Verma, R., Roshan, M. V., Malik, F., Lee, P., Lee, S., Springham, S. V., Tan, T. L., Krishnan, M. and Rawat, R. S. 2008 Compact sub-kilojoule range fast miniature plasma focus as portable neutron source. *Plasma Sources Sci. Technol.* **17**, 045020.

Ziegler, J. F., Biersack, J. P. and Littmark, U. 1985 *The Stopping and Range of Ions in Solids.* New York: Peragomon Press.

https://doi.org/10.1017/S0022377812000190 Published online by Cambridge University Press